PNAS
www.pnas.org

Supplementary Information for

Intraflagellar Transport Protein RABL5/IFT22 Recruits the BBSome to the Basal Body through the GTPase ARL6/BBS3

Bin Xue, Yan-Xia Liu, Bin Dong, Jenna L. Wingfield, Mingfu Wu, Jun Sun, Karl F. Lechtreck and Zhen-Chuan Fan

Zhen-Chuan Fan

Email: fanzhen@tust.edu.cn

This PDF file includes:

Materials and methods
Figures S1 to S6
Tables S1 to S3
Legends for Movies S1 to S8
SI References

Other supplementary materials for this manuscript include the following:

Movies S1 to S8

Materials and methods

Plasmids

Expression vectors were generated on pBKS-gIFT25::HA::GFP-Paro and pBKS-gIFT25::HA::GFP-Ble backbones that contain GFP coding sequences followed immediately downstream by the Rubisco 3'-UTR sequence and the AphVIII cassette (*Paro*, paromomycin resistant gene) or Bleomycin cassette (*Ble*, Zeocine resistant gene) (1). To express IFT22::HA::GFP, a 2,372-bp DNA fragment composing of a 1,235-bp promoter sequence and the *IFT22-HA* coding sequence was amplified from genomic DNA (genomic DNA was prepared using a Genomic DNA Prep kit from Solarbio following the kit's protocol) by using the primer pair (gIFT22-FOR and gIFT22-REV) as listed in Table S2 and was inserted into the *Xba*I and *Eco*RI sites of pBKS-gIFT25::HA::GFP-Paro (1), resulting in pBKS-gIFT22::HA::GFP-Paro. To express IFT22[T19N]::HA::GFP and IFT22[Q69L]::HA::GFP, the amplified DNA fragment as described above was inserted into the *Xba*I and *Eco*RI sites of pBluescript II KS(+) vector and the desiring mutations were introduced by site-directed mutagenesis using the primer pairs (IFT22T19N-FOR and IFT22T19N-REV, IFT22Q69L-FOR and IFT22Q69L-REV) as listed in Table S2. Afterwards, the mutated DNAs were inserted into the *Xba*I and *Eco*RI sites of the pBKS-gIFT25::HA::GFP-Paro vector, resulting in pBKS-gIFT22[T19N]::HA::GFP-Paro and pBKS-gIFT22[Q69L]::HA::GFP-Paro. IFT22::HA, IFT22[T19N]::HA and IFT22[Q69L]::HA sequences were cut from corresponding vectors and inserted into the *Not*I and *Eco*RI sites of pBKS-gIFT25::HA::GFP-Ble, resulting in pBKS-gIFT22::HA::GFP-Ble, pBKS-gIFT22[T19N]::HA::GFP-Ble and pBKS-gIFT22[Q69L]::HA::GFP-Ble, respectively. The *IFT22-mut* sequence was amplified from the genomic DNA of the IFT22 CLiP mutant (LMJ.RY0402.055518) by using the primer pair (gIFT22-FOR and gIFT22-REV) as listed in Table S2. This sequence was inserted into the *Not*I and *Eco*RI sites of pBKS-gIFT25::HA::GFP-Ble, resulting in pBKS-gIFT22-mut::HA::GFP-Ble.

To express BBS3::GFP, a 2,282-bp DNA fragment composing of a 674-bp promoter sequence was amplified from genomic DNA by using the primer pair (gBBS3-FOR and gBBS3-REV) as listed in Table S2 and was inserted into the *Xba*I and *Eco*RI sites of pBKS-gIFT25::HA::GFP-Paro (1), resulting in pBKS-gBBS3::GFP-Paro. To express BBS3[T31R]::GFP, BBS3[A73L]::GFP, the BBS3 DNA fragment amplified above was inserted into the *Xba*I and *Eco*RI sites of pBluescript II KS(+) vector and the desiring mutations were introduced by site-directed mutagenesis using the primer pairs (BBS3T31R-FOR and BBS3T31R-REV, BBS3A73L-FOR and BBS3A73L-REV) as listed in Table S2. The mutated DNAs were inserted into the *Xba*I and *Eco*RI sites of the pBKS-gBBS3::GFP-Paro, resulting in pBKS-gBBS3[T31R]::GFP-Paro, and pBKS-gBBS3[A73L]::GFP-Paro, respectively. The BBS3, BBS3[T31R] and BBS3[A73L] encoding sequences were cut from pBKS-gBBS3::GFP-Paro, pBKS-gBBS3[T31R]::GFP-Paro and pBKS-gBBS3[A73L]::GFP-Paro

and inserted into the *Not*I and *Eco*RI sites of pBKS-gIFT25::HA::GFP-Ble, resulting in pBKS-gBBS3::GFP-Ble, pBKS-gBBS3[T31R]::GFP-Ble and pBKS-gBBS3[A73L]::GFP-Ble, respectively.

To express BBS5::YFP, a 4,028-bp DNA fragment composing of a 1,197-bp promoter sequence and the *BBS5* coding sequence was amplified from genomic DNA using primer pair (gBBS5-FOR and gBBS5-REV) as listed in Table S2 and inserted into the *Not*I and *Bam*HI sites of pBluescript II KS(+) vector, resulting in pBKS-gBBS5. Afterwards, *BBS5* sequence was cut from pBKS-gBBS5, and inserted into the *Not*I and *Eco*RI sites of pBKS-gIFT22::HA::GFP-Paro and pBKS-gIFT22::HA::GFP-Ble, resulting in pBKS-gBBS5::GFP-Paro and pBKS-gBBS5::GFP-Ble, respectively. YFP was amplified from pHK214 (2) by using the primer pair (GFP-FOR and GFP-REV) as listed in Table S2 with *Eco*RI and *Xho*I restriction enzyme sites located in its 5'- and 3'-end, respectively, and inserted into *Eco*RI and *Xho*I sites of pBKS-gBBS5::GFP-Paro and pBKS-gBBS5::GFP-Ble, resulting in pBKS-gBBS5::YFP-Paro and pBKS-gBBS5::YFP-Ble, respectively. The miRNA targeting 3'-UTRs of *IFT22* and *BBS3* were designed using WMD3 software (http://wmd3.weigelworld.org) according to a previously described method (3). Briefly, the output oligonucleotide was combined with the miRNA cre-MIR1157 (accession number MI0006219), resulting in miRNA precursor sequences of 171-bp for *IFT22* and *BBS3* (Table S2). The sequences were synthesized by Genewiz (China) and ligated to the *Eco*RV and *Eco*RI sites of pHK263 plasmid (3), resulting in pMi-IFT22-Paro and pMi-BBS3-Paro, respectively. All new vectors were verified by direct nucleotide sequencing.

Transgenic strain generation

C. reinhardtii was transformed with the constructed vectors as shown above by the electroporation method as described previously (4) and the transformants were selected on TAP plates with 20 µg/ml paromomycin (Sigma-Aldrich), 15 µg/ml bleomycin (Invitrogen) or both antibiotics with 10 µg/ml paromomycin and 5 µg/ml bleomycin. The positive transformants were identified and the target proteins were quantified directly by immunoblotting as described below. The screening of IFT22 and BBS3 miRNA cells was initiated by checking the cellular level of the target protein through immunoblotting of whole cell extracts with IFT22 and BBS3 antibodies. The miRNA strains showing a reduced level of the target protein were selected for further phenotypic analysis.

Antibodies and immunoblotting

Rabbit-raised polyclonal antibodies against IFT25, IFT46, IFT57, IFT70, IFT139 have been reported previously (1). Rabbit-originated antibodies against IFT22, BBS1, BBS3 and BBS5 were generated by Beijing Protein Innovation, LLC (Beijing) (*SI Appendix*, Fig. S6). Rabbit-raised polyclonal anti-IFT43 antibody was reported previously (5). Antibodies against HA (rat 3F10, Roche), GFP (mAbs 7.1 and 13.1, Roche), α-tubulin (mAb B512, Sigma-Aldrich), Ac-tubulin (mAb

6-11B-1, Sigma-Aldrich) and goat anti-mouse, anti-rat and anti-rabbit IgG conjugated to horseradish peroxidase (The Jackson Labs) were commercially available. After whole cell and isolated cell body and cilia samples were boiled for 5 min in Laemmli SDS sample buffer SDS-PAGE electrophoresis and immunoblotting was performed as described previously (6). If not otherwise specified, 20 µg of total protein from each sample was loaded for SDS-PAGE electrophoresis. Quantification of the target proteins was performed by measuring the intensity of the immunoblots with ImageJ software (version 1.42g, National Institutes of Health) and defined as $(MI_{band}-MI_{background})*Pixels_{band}$. MI_{band} and $MI_{background}$ stand for the mean intensity of a target band and the area around a target band, respectively. The intensity of immunoblots was normalized to the intensity of a loading control protein. The data was processed with Prism 7.04 (GraphPad Software). In immunoblotting assays, a dilution used for primary and secondary antibodies was listed in Table S3.

Isolation of cilia and cell bodies

Isolation of cilia and cell bodies were performed according to our protocol reported previously (7). Briefly, 20 liters of cells were concentrated by centrifugation (1,100 ×*g* at room temperature for 2 min) and washed with TAP (pH 7.4) and resuspended in 150 ml of TAP. The collected cells were incubated for 2~4 h under strong light with bubbling. Then, 0.5 M acetic acid was added to reach a pH value of 4.5 and maintained for 1 min to deciliate cells before 0.5 M KOH was added to reach a pH value of 7.4. Next, cells were spun down by centrifugation (600 ×*g* at 4°C for 5 min). The pellets and the supernatants were collected for cell body and cilia, respectively. The supernatants were repeatedly washed with HMDEK (10 mM Hepes, pH 7.4, 5 mM MgSO4, 1 mM DTT, 5 mM EDTA, and 25 mM KCl) by centrifugation (14,000 ×*g* at 4°C for 10 min) until the green color disappeared completely.

Messenger RNA quantification

Quantification of BBS3 mRNA was performed according to our protocol reported previously (1). In brief, 5 µg of RNA was reverse transcribed at 42 °C for 1 h using M-MLV Reverse Transcriptase (Promega) and oligo(T)18 primers (Takara). Relative transcript amounts were measured by SYBR-green quantitative PCR (qPCR) using primer pairs targeting *BBS3* (qBBS3-FOR and qBBS3-REV) (Table S2) with a Mastercycler pro real-time PCR system (Eppendorf). The PCR reactions were performed at 95 °C for 30 sec followed by 40 cycles of 95 °C for 5 sec, 60 °C for 30 sec, and 72 °C for 10 sec. Samples were normalized using guanine nucleotide-binding protein subunit beta-like protein (GBLP) as a housekeeping gene internal control. The primer pair (qGBLP-FOV and qGBLP-REV) was listed in Table S2. Three sets of mRNAs were independently isolated and quantified three times each. Data was analyzed with Prism 7.04 (GraphPad Software).

Immunoprecipitation

Cell bodies and cilia isolated from transformants and control cells were resuspended in HMEK (10 mM Hepes, pH 7.4, 5 mM MgSO4, 5 mM EGTA, and 25 mM KCl) plus protein inhibitors (1 mM PMSF, 50 μg/ml soybean trypsin inhibitor, 1 μg/ml pepstatin A, 2 μg/ml aprotinin, and 1 μg/ml leupeptin) supplemented with 50 mM NaCl and lysed by adding nonidet P-40 (NP-40) to 1%. The supernatants were collected by centrifugation (14,000 ×*g*, 4 °C, 10 min) and were incubated with agitation with 5% BSA-pretreated camel anti-GFP antibody-conjugated agarose beads (V-nanoab Biotechnology) for 2 h at 4 °C. The beads were then washed with HMEK containing 150 mM NaCl, 50 mM NaCl and finally 0 mM NaCl. The beads were then added with Laemmli SDS sample buffer and boiled for 5 min before centrifuging at 2,500 ×*g* for 5 min. The supernatants were then analyzed by immunoblotting as described above. If necessary, the assay was carried out in the presence of GTPγS (20 mM) or GDP (20 mM).

Immunofluorescence

Immunofluorescence assay was carried out according to our protocol reported previously (1). The primary antibodies against GFP, IFT46, BBS3, BBS5 and IFT22 have been described in the antibodies section above. The secondary antibodies were Alexa-Fluor 594 conjugated goat anti-rabbit IgG, Alexa-Flour 488 conjugated goat anti-mouse IgG and Alexa-Flour 488 conjugated goat anti-rabbit IgG (Molecular Probes). Images were obtained using an IX83 inverted fluorescent microscopy (Olympus) equipped with a back illuminated scientific CMOS camera (Prime 95B, Photometrics) at 100× amplification and processed with CellSens Dimension (version 2.1, Olympus) and ImageJ software (version 1.42g, National Institutes of Health). Contrasts were adjusted identically for each series of panels. A dilution used for primary and secondary antibodies was listed in Table S3.

IFT video imaging and speed and frequency measurements

The ciliary motility of GFP- and YFP-tagged proteins was imaged at ~15 frames per second (fps) using total internal reflection fluorescence (TIRF) microscopy on an inverted microscope (IX83, Olympus) equipped with a through-the-objective TIRF system, a 100×/1.49 NA TIRF oil immersion objective (Olympus), and a back illuminated scientific CMOS camera (Prime 95B, Photometrics) as detailed previously (8, 9). To quantify IFT speeds and frequencies, kymogram were generated and measured with CellSens Dimension (version 2.1, Olympus). In the kymogram, anterograde transports result in diagonal trajectories from the middle to both sides; trajectories of retrograde transports run from both sides to the middle.

Purification of bacterial-expressed proteins

IFT22, IFT22-mut and BBS3 cDNAs were amplified from total RNA of *Chlamydomonas* using the

primer pairs (cIFT22-FOR and cIFT22-REV for IFT22 and IFT22-mut cDNAs, cBBS3-FOR and cBBS3-REV for BBS3 cDNA) as listed in Table S2. The desiring mutations in IFT22 and BBS3 encoding cDNA were introduced by site-directed mutagenesis using the primer pairs as listed in Table S2. The cDNAs encoding IFT22, BBS3 and their mutants were inserted into the *Eco*RI and *Xho*I sites of pET30a (Novagen) and the *Bam*HI and *Hin*dIII sites of pGEX-6P (Amersham Biosciences) to result in a total of six plasmids (1). IFT22 and its mutants were expressed as N-terminal 6×His-tagged proteins and BBS3 and its mutants were expressed as proteins with an N-terminal GST tag. Bacterial-expressed recombinant proteins were purified with Ni-NTA (IFT22 and its mutants) beads and cleaved with thrombin (Solarbio) to get rid of the N-terminal 6×His tag. These proteins were mixed with the N-terminal GST tagged BBS3 and its mutants or GST, which were purified with glutathione sepharose beads. According to the experiments, glutathione sepharose purification was performed on the mixture as described previously (10). Ten micrograms of proteins from elutes were resolved on 12% SDS-PAGE gels and visualized with Coomassie Blue staining. If necessary, the assay was carried out in the presence of GTPγS (20 mM), GDP (20 mM) or EDTA (20 μM).

Small GTPase assay

N-terminal 6×His tagged IFT22 (6×His::IFT22), IFT22[Q69L] (6×His-IFT22[Q69L]) or IFT22[T19N] (6×His-IFT22[T19N]) were expressed in bacteria and used for affinity purification with Ni-NTA resin as described above. IFT22 or its mutants were loaded with at least a 25-fold molar excess of GTP at room temperature for 1 h in the incubation buffer (20 mM HEPES pH7.5, 150 mM NaCl, 5 mM EDTA and 1 mM dithiothreitol). The beads were washed for five times before the purified proteins were eluted. Free nucleotide was removed with 10 ml G25-resin (GE Healthcare) pre-equilibrated with 20 mM HEPES pH 7.5, 150 mM NaCl. The intrinsic and GAP-accelerated GTP hydrolysis was measured by an optical assay for the release of inorganic phosphate with the use of reagents from the QuantiChrom™ ATPase/GTPase assay kit (Bioassay Systems) (11). In detail, 10 μl (20 μM) GTP-loaded proteins were mixed with 20 μl of 2× assay buffer solutions. Ten micro-litter distilled water, cell body extracts or ciliary extracts of *Chlamydomonas* was further added for the measurement of intrinsic or GAP-accelerated GTP hydrolysis. The reaction was dispensed into 96-well half-area microplates (Corning) and performed at room temperature for 0, 15, 30, 60 and 120 min, respectively. After that, 200 μl reagent solutions were added to each reaction and allowed to incubate for 30 min at room temperature. The absorbance at 620 nm was measured with a synergy H1/MF microplate reader (Bio-Tek). The values shown were calculated from data derived from three independently-generated experiments. Preparation of cell body and ciliary extracts of *Chlamydomonas* has been described previously (10). The chlorophy11- and GTP-contaminants were removed by applying the extracts through the G25 resin (GE Healthcare). The free phosphate was removed with a Pi-Bind resin (Innova Biosciences). The cell body extracts were diluted with

lysis buffer to a final concentration of 1 mg protein/ml to avoid the effect of chlorophy11 on the absorbance.

Sucrose density gradient centrifugation of ciliary extracts

Linear 12 ml 10-25% sucrose density gradients in 1×HMDEK buffer plus protease inhibitors (1 mM PMSF, 50 μg/ml soybean trypsin inhibitor, 1 μg/ml pepstatin A, 2 μg/ml aprotinin, 1 μg/ml leupeptin) and 1% NP-40 were generated by using the Jule Gradient Former (Jule, Inc. Milford) and used within 1 hour. Cilia were opened by liquid nitrogen for three rounds of frozen-and-thaw cycles and centrifuged at 12,000 rpm, 4 °C, for 10 min. 700 μl of ciliary extracts were then loaded on the top of the gradients and separated at 38,000 rpm, 4°C, for 14 hours in a SW41Ti rotor (Beckman Coulter). The gradients were fractioned into 24 to 26 0.5 ml aliquots by using a Pharmacia LKB Pump P-1 coupled with a FRAC-100 fraction collector. The standards used to calculate S-values were BSA (4.4S), aldolase (7.35S), catalase (11.3S), and thyroglobulin (19.4S). Twenty micro-liters of each fraction was analyzed by immunoblotting as described above.

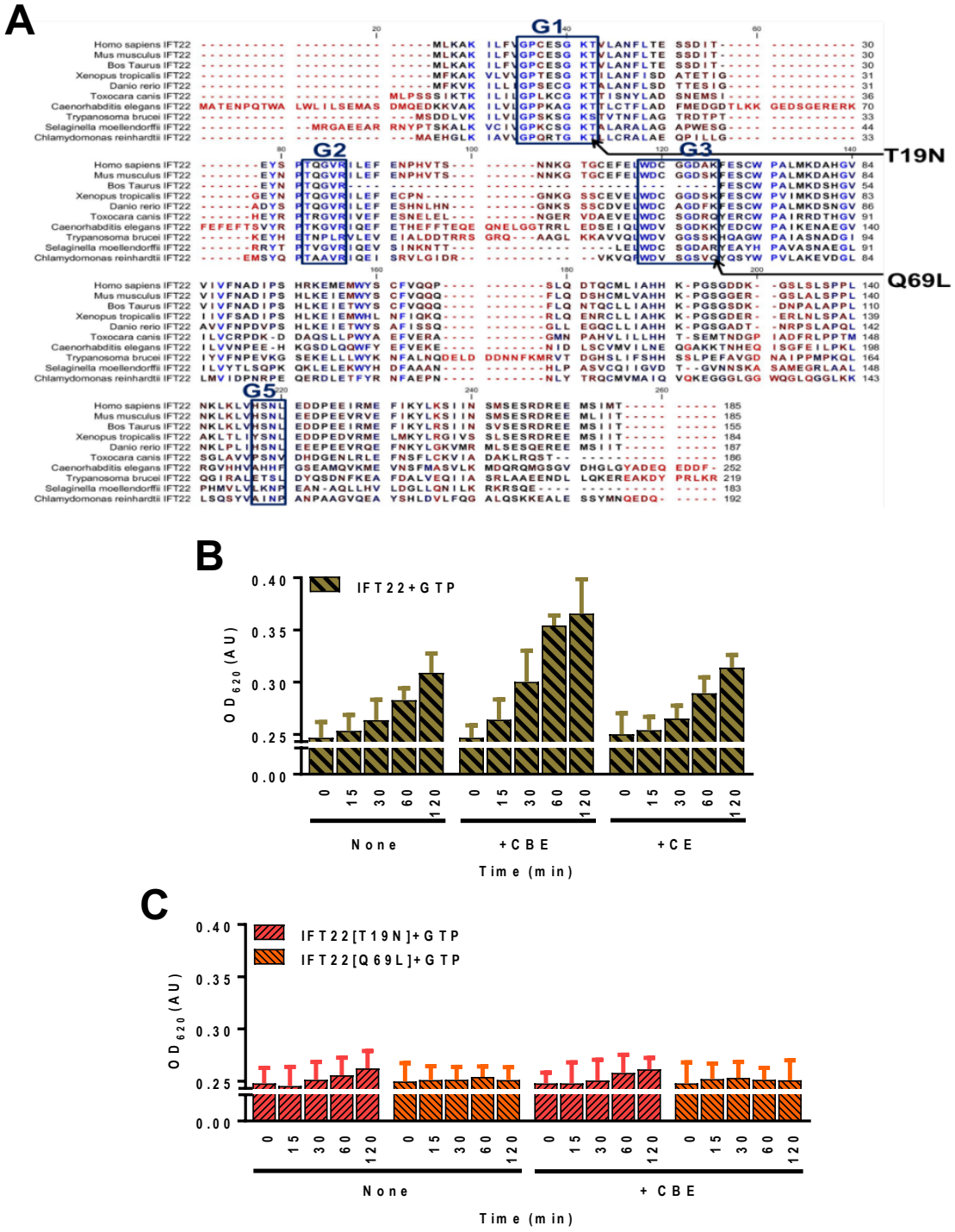

Fig. S1. IFT22 is a highly conserved protein across ciliated species and is an active GTPase with low intrinsic GTPase activity. (A) Sequence alignment of deduced amino acid sequences from ten invertebrate and vertebrate IFT22 orthologues and modified IFT22 sequences. Alignments were generated using CLC main workbench (version 6.8); the most conserved residues are shown in blue, the least conserved are in red. IFT22 contains four conserved domains including G1, G2, G3

and G5 as labeled in the boxes. The P-loop threonine (T19) and glutamine (Q69) were marked. Dashes indicate gaps introduced to optimize the alignment. Arrowheads indicate missense mutations created in possible dominant-negative and constitutive-active IFT22 mutants. Accession numbers are as follows: *Homo sapiens*, NP_073614.1, *Mus musculus*, AAH09150.1, *Bos Taurus*, AAI02615.1, *Xenopus tropicalis*, NP_001011271.1, *Danio rerio,* NP_001017884.1, *Toxocara canis*, KHN79365.1, *Caenorhabditis elegans*, NP_503073.1, *Trymanosoma brucei*, EAN80628.1, *Selaginella moellendorffii*, XP_002975921.1, and *Chlamydomonas reinhardtii*, XP_001689669.1. (B) GTP hydrolysis of IFT22 in the absence and presence of cell body extracts (CBE) and ciliary extracts (CE) isolated from CC-125 cells. IFT22 shows low intrinsic GTPase activity. The presence of CBE but not CE elevates the GTPase activity of IFT22. (C) GTP hydrolysis of IFT22[T19N] and IFT22[Q69L] in the absence (None) and presence of CBE of CC-125 cells. In the absence of CBE, introduction of a leucine at the position of Q69 of IFT22 reduces the intrinsic GTPase activity (also see Fig. S1B). In contrast, the presence of CBE does not elevate the GTPase activity of IFT22[Q69L], indicating that IFT22[Q69L] appears to be a GTPase activating protein (GAP)-resistant variant. As for IFT22[T19N], no GTPase activity was observed no matter if CBE was present or not. For panels B and C, the assay was performed in a time-course pattern as shown and the inorganic phosphate (Pi) release upon GTP hydrolysis is measured by absorbance at 620 nm. The background absorbance was measured using Pi-free buffer alone or Pi-free buffer plus the purified cell extracts.

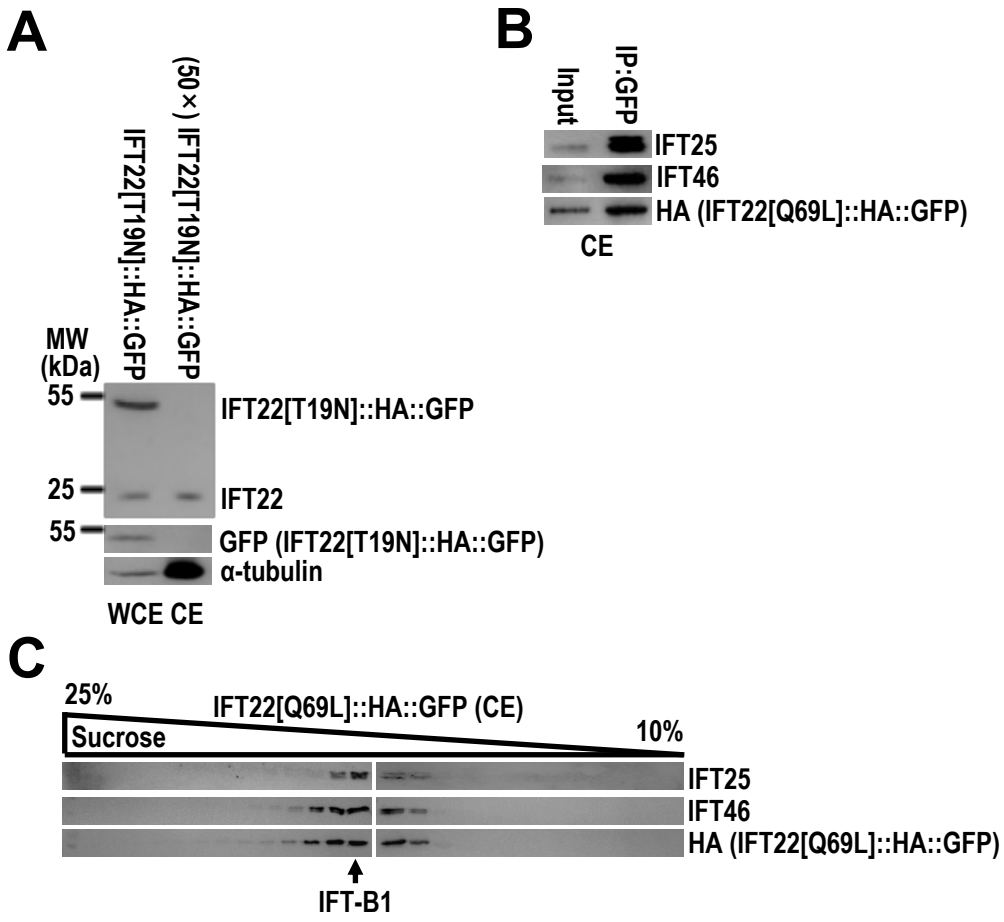

Fig. S2. IFT22 binds IFT-B1 as its effector for ciliary entry. (A) Immunoblots of whole cell extracts (WCE) and CE of IFT22[T19N]::HA::GFP cells probed with α-IFT22 and α-GFP. Fifty times more protein of CE than WCE proteins were loaded in the SDS-PAGE. IFT22[T19N]::HA::GFP does not enter cilia. Alpha-tubulin was used to adjust the loading. (B) Immunoblots of α-GFP captured proteins from CE of IFT22[Q69L]::HA::GFP cells probed with α-IFT25, α-IFT46 and α-HA. The IFT-B1 subunits IFT25 and IFT46 are immunoprecipitated with IFT22[Q69L]::HA::GFP. (C) Immunoblots of CE of IFT22[Q69L]::HA::GFP cells separated by sucrose density gradient centrifugation probed with α-IFT25, α-IFT46 and α-HA. IFT22[Q69L]::HA::GFP co-sediments with the IFT-B1 subunits IFT25 and IFT46

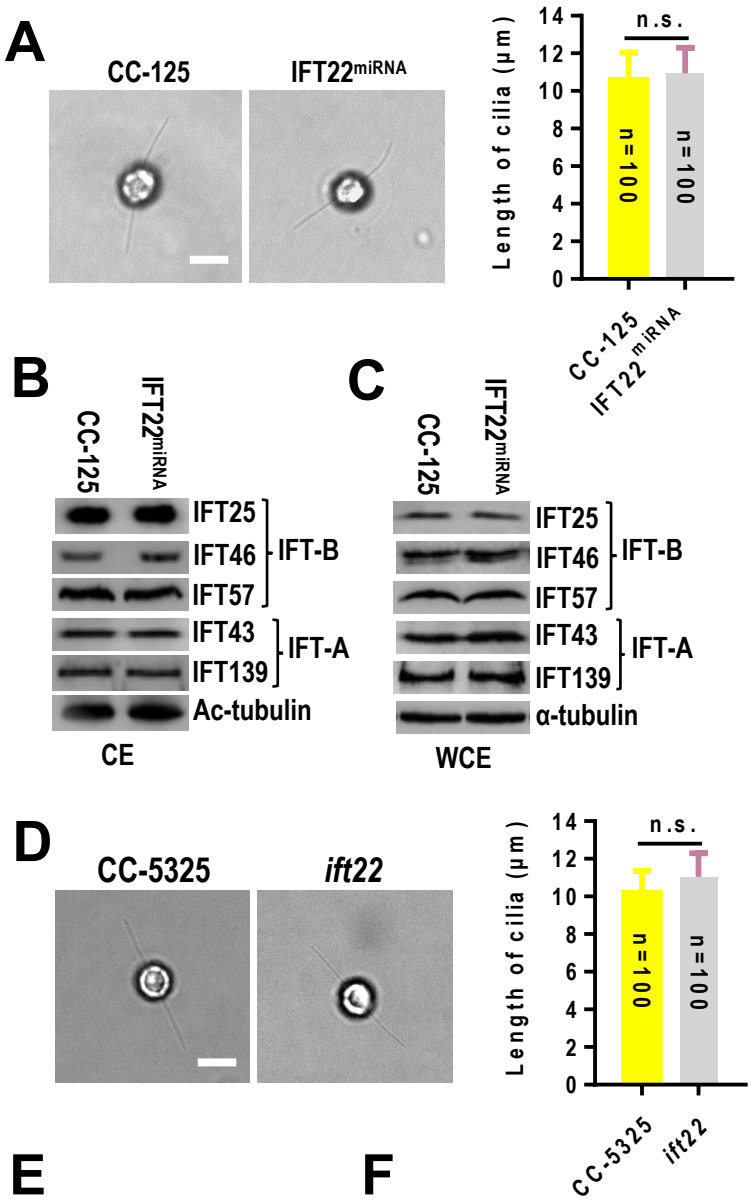
A
CC-125
IFT22miRNA
Length of cilia (μm)
n.s.
n=100
n=100
CC-125
IFT22 miRNA
B
CC-125
IFT22miRNA
IFT25
IFT46
IFT57
IFT-B
IFT43
IFT139
IFT-A
Ac-tubulin
CE
C
CC-125
IFT22miRNA
IFT25
IFT46
IFT57
IFT-B
IFT43
IFT139
IFT-A
α-tubulin
WCE
D
CC-5325
ift22
Length of cilia (μm)
n.s.
n=100
n=100
CC-5325
ift22
E
CC-5325
ift22
IFT25
IFT46
IFT57
IFT-B
IFT43
IFT139
IFT-A
α-tubulin
WCE
F
CC-5325
ift22
IFT25
IFT46
IFT57
IFT-B
IFT43
IFT139
IFT-A
Ac-tubulin
CE

Fig. S3. IFT22 is not required for maintaining ciliary length and IFT protein abundance. (A) Phase contrast images of CC-125 and IFT22^{miRNA} cells. IFT22^{miRNA} cells had full-length cilia (10.94 ± 1.35 μm) compared to CC-125 cells (10.63 ± 1.41 μm). (B&C) Immunoblots of CE (B) and WCE (C) of CC-125 and IFT22^{miRNA} cells probed for the IFT-B proteins IFT25, IFT46 and IFT57 and the IFT-A proteins IFT43 and IFT139. Knockdown of IFT22 does not cause changes on cellular and ciliary levels of these IFT proteins as compared to that of CC-125 cells. (D) Phase contrast images of CC-5325 and *ift22* cells. The *ift22* cells had full-length cilia (10.98 ± 1.19 μm) compared to CC-5325 cells (11.11 ± 1.61 μm). (E&F) Immunoblots of WCE (E) and CE (F) of CC-5325 and *ift22* cells probed for IFT25, IFT46, IFT57, IFT43 and IFT139. The loss of IFT22 in cilia does not affect the cellular and ciliary abundance of these IFT proteins. For panels A and D, the data shown was calculated from 100 cilia (n=100 repeats). Scale bars: 5 μm. For panels B&C and E&F, alpha-tubulin and Ac-tubulin were used to adjust the loading for WCE and CE, respectively.

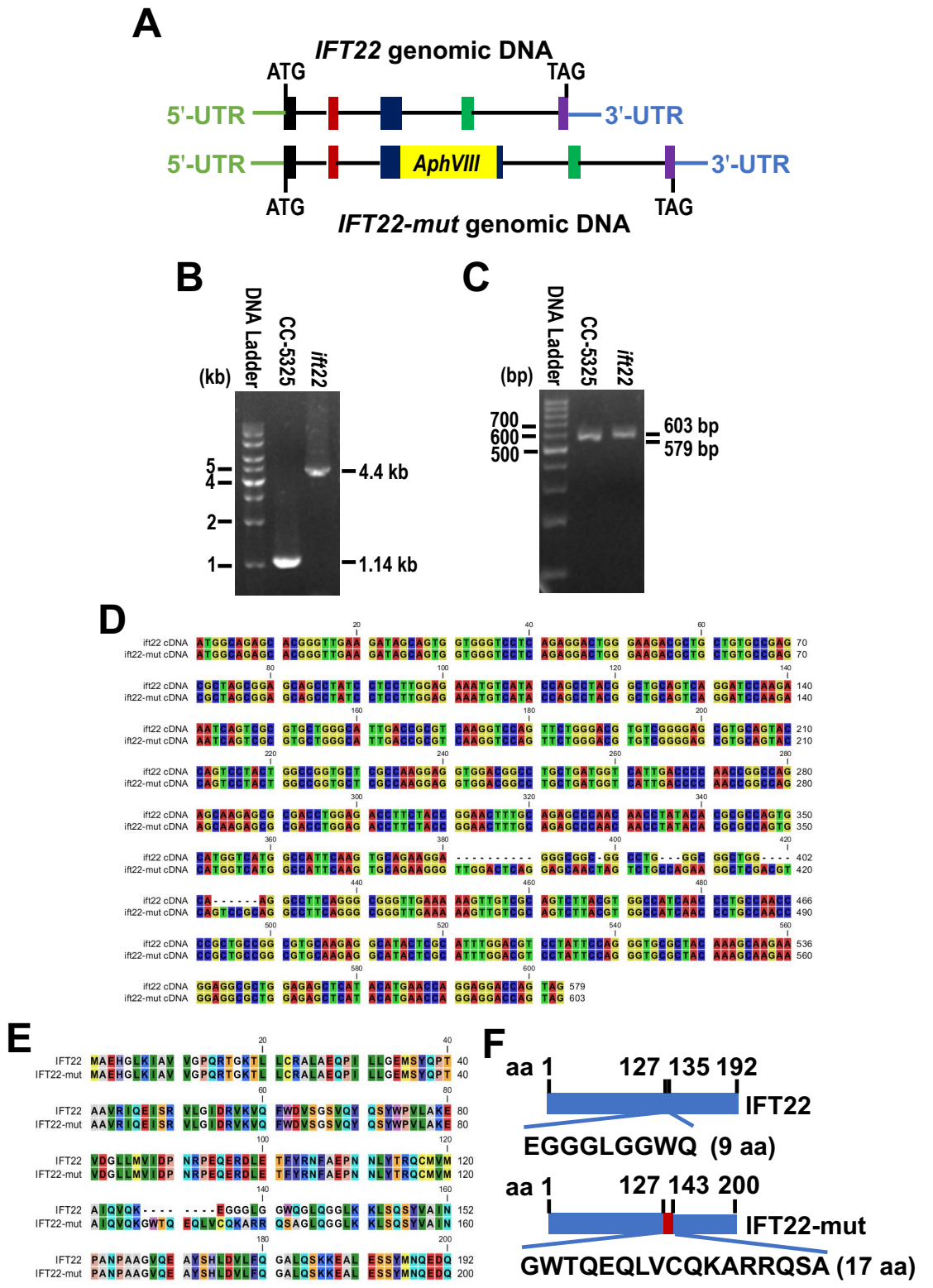

Fig. S4. Characterization of the IFT22 CLiP strain (LMJ.RY0402.055518). (A) A paromomycin-resistant gene (*AphVIII*) inserted at 3'- proximal region of the third exon in *IFT22* gene of the *ift22* cells. The boxes with colors and the lines represent the exons and introns of *IFT22* gene,

respectively. (B) Agarose gel electrophoresis of the PCR products amplified from genomes of CC-5325 and *ift22* cells. The primer pair cIFT22-FOR and cIFT22-REV were used to amplify the *IFT22* genomic DNA of 1,140-bp from CC-5325 cells. A single DNA fragment of ~4.4-kb (4,428-bp) was amplified from the *ift22* cells by using the same primer pair. (C) Agarose gel electrophoresis of *IFT22* cDNAs amplified from CC-5325 and *ift22* cells. A single cDNA band of 579- and 603-bp was amplified from CC-5325 and *ift22* cells, respectively. (D) Sequence alignment of the *IFT22* cDNAs between CC-5325 and *ift22* cells. The *ift22* cells contain a mutated *IFT22* cDNA (shown as ift22-mut cDNA) 24 base pair longer than the wild-type *IFT22* cDNA (shown as ift22 cDNA). (E) Sequence alignment of IFT22 proteins between CC-5325 and *ift22* cells. The *ift22* cells produce an IFT22 mutant protein (shown as IFT22-mut) eight acids longer than the wild-type IFT22 protein (shown as IFT22). (F) In the IFT22-mut protein, the 9 amino-acid sequence EGGGLGGWQ (amino acids 127 to 135 of IFT22) was replaced with a 17 amino-acid sequence GWTQEQLVCQKARRQSA (amino acids 127 to 143 of IFT22-mut).

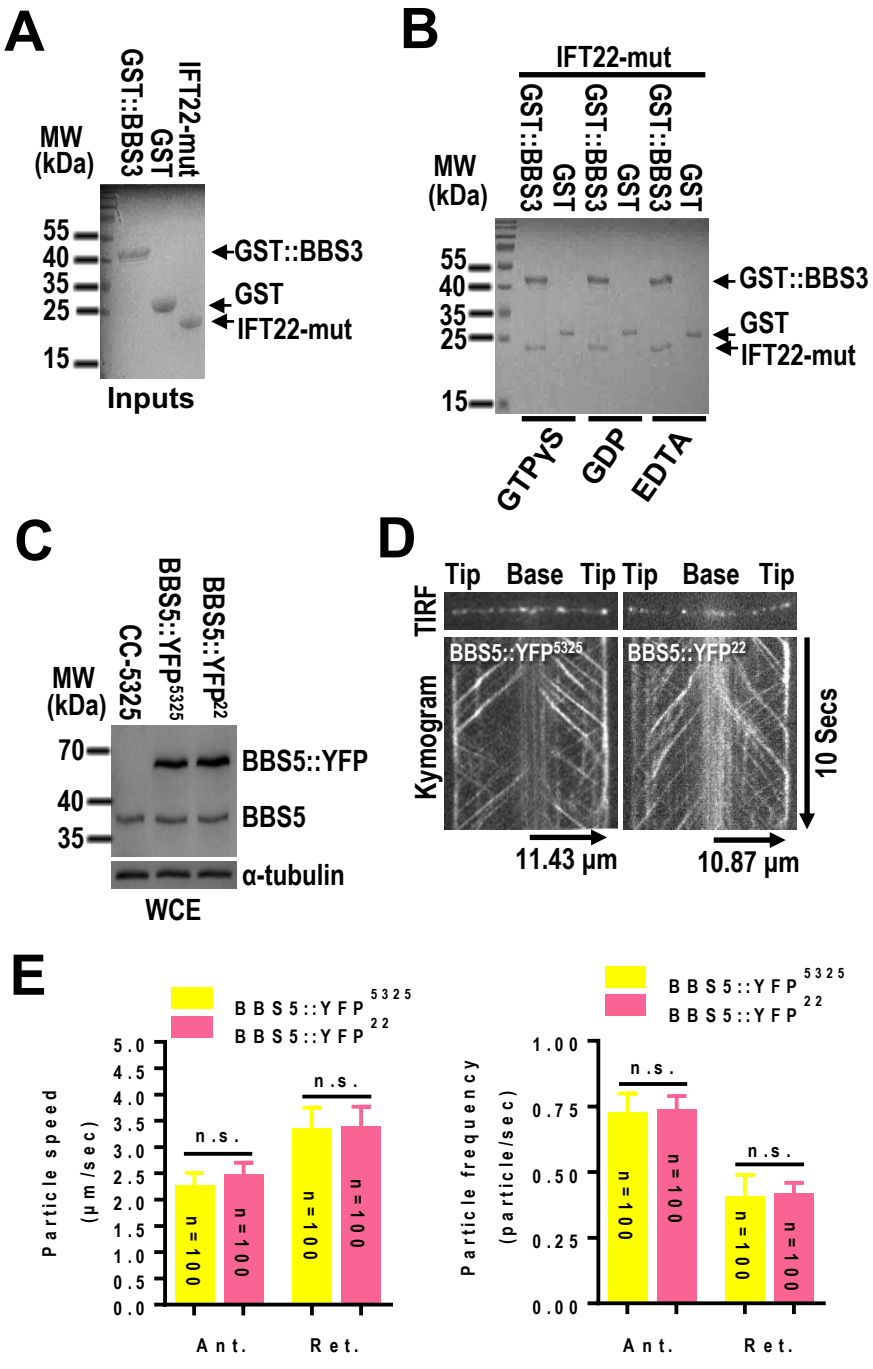

Fig. S5. IFT22-mut binds BBS3 and ciliary cycling of the BBSome does not require IFT22. (A) Bacterial-expressed IFT22-mut, GST, and GST::BBS3 purified to near-homogeneity before SDS-PAGE and Coomassie staining. (B) IFT22-mut mixed with GST::BBS3 or GST in the presence of GTPγS, GDP or EDTA and complexes recovered on Glutathione beads before elution, SDS-PAGE, and Coomassie staining. Under all three conditions, IFT22-mut binds GST::BBS3 but not GST alone. (C) Immunoblots of WCE of CC-5325, BBS5::YFP^{5325} and BBS5::YFP^{22} cells probed with α-

BBS5. Similar amounts of BBS5::YFP are expressed in two strains. (D) TIRF images and corresponding kymograms of BBS5::YFP^{5325} and BBS5::YFP^{22} cells. In the kymograms, the time and transport lengths are indicated on the *Right* and on the *Bottom*, respectively. (E) The speeds and frequencies of the BBS5::YFP in cilia of BBS5::YFP^{5325} and BBS5::YFP^{22} cells were listed in the graph. The speeds of BBS5::YFP in cilia of BBS5::YFP^{22} cells were 2.48 ± 0.22 (n=100) and 3.4 ± 0.37 μm/s (n=100) for anterograde and retrograde, respectively, similar to that (2.27 ± 0.24 μm/s, n=100 and 3.35 ± 0.4 μm/s, n=100 for anterograde and retrograde, respectively) in cilia of BBS5::YFP^{5325} cells. The frequencies of BBS5::YFP in cilia of BBS5::YFP^{22} cells were 0.74 ± 0.05 particles/s (n=100) and 0.42 ± 0.04 particles/s (n-100) for anterograde and for retrograde, respectively, similar to that (0.73 ± 0.07 particles/s, n=100 and 0.41 ± 0.08 particles/s, n=100 for anterograde and retrograde, respectively) in cilia of BBS5::YFP^{5325} cells. Ant. and Ret. represent anterograde and retrograde, respectively.

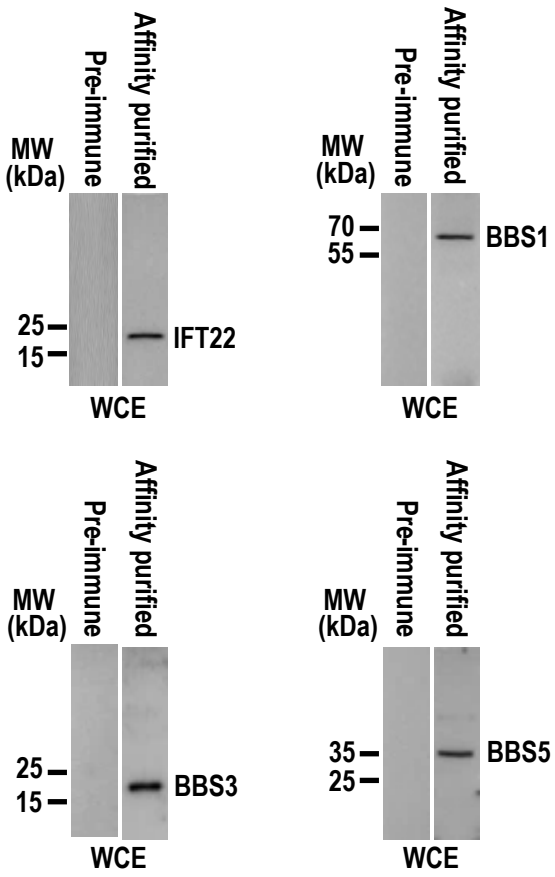

Fig. S6. Affinity-purified polyclonal antisera against IFT22, BBS1, BBS3 and BBS5 can recognize their target proteins specifically. Immunoblots of WCE isolated from CC-125 cells with the affinity-purified IFT22, BBS1, BBS3 or BBS5 antisera identified one band with a size of approximately 22, 63, 20 or 39 kDa as expected, respectively. In contrast, the pre-immune serum does not recognize any specific bands. MW stands for molecular weight.

Table S1. *Chlamydomonas* strains used in this study

Name	Vector/background strain	Reference or source
CC-125	Wild-type strain	*Chlamydomonas* Genetic Center
CC-5325	Wild-type strain	*Chlamydomonas* Genetic Center
ift22	IFT22 CLiP mutant/CC-5325 (LMJ.RY0402.055518)	*Chlamydomonas* Genetic Center
IFT22::HA::GFP	pBKS-gIFT22::HA::GFP-Paro/CC-125	This study
IFT22[T19N]::HA::GFP	pBKS-gIFT22[T19N]::HA::GFP-Paro/CC-125	This study
IFT22[Q69L]::HA::GFP	pBKS-gIFT22[Q69L]::HA::GFP-Paro/CC-125	This study
$IFT22^{miRNA}$	pMi-IFT22-Paro/CC-125	This study
$IFT22^{Res\text{-}WT}$	pBKS-gIFT22::HA::GFP-Ble/$IFT22^{miRNA}$	This study
$IFT22^{Res\text{-}T19N}$	pBKS-gIFT22[T19N]::HA::GFP-Ble/$IFT22^{miRNA}$	This study
$IFT22^{Res\text{-}Q69L}$	pBKS-gIFT22[Q69L]::HA::GFP-Ble/$IFT22^{miRNA}$	This study
$IFT22^{Res\text{-}22\text{-}mut}$	pBKS-gIFT22-mut::HA::GFP-Ble/$IFT22^{miRNA}$	This study
$BBS3^{miRNA}$	pMi-BBS3-Paro/CC-125	This study
$BBS3^{Res\text{-}WT}$	pBKS-gBBS3::GFP-Ble/$BBS3^{miRNA}$	This study
$BBS3^{Res\text{-}T31R}$	pBKS-gBBS3[T31R]::GFP-Ble/$BBS3^{miRNA}$	This study
$BBS3^{Res\text{-}A73L}$	pBKS-gBBS3[A73L]::GFP-Ble/$BBS3^{miRNA}$	This study
BBS5::YFP	pBKS-gBBS5::YFP-Paro/CC-125	This study
$BBS5::YFP^{22miRNA}$	pBKS-gBBS5::YFP-Ble/$IFT22^{miRNA}$	This study
$BBS5::YFP^{3miRNA}$	pBKS-gBBS5::YFP-Ble/$BBS3^{miRNA}$	This study
$BBS5::YFP^{5325}$	pBKS-gBBS5::YFP-Ble/CC-5325	This study
$BBS5::YFP^{22}$	pBKS-gBBS5::YFP-Ble/*ift22*	This study

Table S2. Primers used in this study

Name	Nucleotide sequence
Primers used to clone target genes	
gIFT22-FOR	5'-GCTCTAGATACCGCGATCAAAGCACACTC-3'
gIFT22-REV	5'-GGAATTCGGCGTAGTCGGGCACGTCGTAGGGG TACTGGTCCTCCTGGTTCATGTATG-3'
gBBS3-FOR	5'-GCTCTAGATTCCCACTCCCGCAGCC-3'
gBBS3-REV	5'-GGAATTCGCTGAGGCGCTCCGCC-3'
gBBS5-FOR	5'-CCGCGGCCGCGCTCCGGCTGAACGGTCCTCCCG-3'
gBBS5-REV	5'-CCGGATCCCAGCACGCTCCACAGCTGCTCCACC-3'
GFP-FOR	5'-CGGAATTCATGGCCAAGGGCGAGG-3'
GFP-REV	5'-CCGCTCGAGTTACTTGTACAGCTCGTCCATGC-3'
cIFT22-FOR	5'-CGGAATTCATGGCAGAGCACGGGTTG-3'
cIFT22-REV	5'-CCGCTCGAGTTACTGGTCCTCCTGGTTC-3'
cBBS3-FOR	5'- CGGGATCCATGGGCTTCTTTGACAAGCT-3'
cBBS3-REV	5'- CCCAAGCTTTTAGCTGAGGCGCTCCG-3'
Primers used to do site-directed mutagenesis	
IFT22Q69L-FOR	5'-GAGCGTGCTGTACCAGTCCTACT-3'
IFT22Q69L-REV	5'-CTCGCACGACATGGTCAGGATGA-3'
IFT22T19N-FOR	5'-AGAGGACTGGGAAGAACCTGCTGTG-3'
IFT22T19N-REV	5'-TCTCCTGACCCTTCTTGGACGACAC-3'
BBS3T31R-FOR	5'-CAGCGGCAAGCGCACGATCATTG-3'
BBS3T31R-REV	5'-GTCGCCGTTCGCGTGCTAGTAAC-3'
BBS3A73L-FOR	5'-CATGTCCGGCCTGGGGAGATACC-3'
BBS3A73L-REV	5'-GTACAGGCCGGACCCCTCTATGG-3'
Primers used to quantify mRNA levels	
qGBLP-FOR	5'-GTCATCCACTGCCTGTGCTTCT-3'
qGBLP-REV	5'-GGCCTTCTTGCTGGTGATGTT-3'
qBBS3-FOR	5'-GAGATACCGGACGCTGTGG-3'
qBBS3-REV	5'-GGGCAGGTCCTTCTTATTGG-3'
Primers used to generate IFT22 and BBS3 miRNA constructs	
IFT22 miRNA	5'-GATATCAGGAAACCAAGGCGCGCTAGCTTCCTGGGCGCAGT GTTCCAGCTGCAGTACTGATTAAGCGTATCCTCCCAGCTCGCTG ATCGGCACCATGGGGGTGGTGGTGATCAGCGCTACTGGGAGGAT ACGCTTAATCATACTGCAGCCGGAACACTGC CAGGAGAATTC-3'
BBS3 miRNA	5'-GATATCAGGAAACCAAGGCGCGCTAGCTTCCTGGGCGCAGTG TTCCAGCTGCAGTACTCTATAACGTCAATACGACACCTCGCTGC TCGGCACCATGGGGGTGGTGGTGATCAGCGCTAGTGTCGTATTG ACGTTATAGATA CTGCAGCCGGAACACTGCCAGGAGAATTC-3'

Table S3. Antibodies used in this study

Antibody	Dilution		Origins	Reference or source
	IB	IF		
Anti-IFT22	1:1,000	1:100	Rabbit	This study
Anti-IFT25	1:1,000	N/A	Rabbit	(1)
Anti -IFT46	1:1,000	1:100	Rabbit	(1)
Anti-IFT70	1:1000	N/A	Rabbit	(1)
Anti-IFT57	1:1,000	N/A	Rabbit	(1)
Anti-IFT43	1:500	N/A	Rabbit	(5)
Anti-IFT139	1:1,000	N/A	Rabbit	(1)
Anti-BBS1	1:1,000	N/A	Rabbit	This study
Anti-BBS3	1:500	1:25	Rabbit	This study
Anti-BBS5	1:1000	1:50	Rabbit	This study
Anti-α-tubulin	1:10,000	N/A	Mouse	Sigma-Aldrich
Anti-acetylated-tubulin	1:30,000	N/A	Mouse	Sigma-Aldrich
Anti-GFP	1:1,000	1:50	Mouse	Roche
Anti-HA	1:1,000	N/A	Rat	Roche
HRP-conjugated goat anti-mouse IgG	1:10,000	N/A	Goat	The Jackson Lab.
HRP-conjugated goat anti-rat IgG	1:10,000	N/A	Goat	The Jackson Lab.
HRP-conjugated goat anti-rabbit IgG	1:10,000	N/A	Goat	The Jackson Lab.
Alexa-Fluor 594-conjugated goat anti-rabbit IgG	N/A	1:400	Goat	Molecular Probes
Alexa-Flour 488-conjugated goat anti-mouse IgG	N/A	1:400	Goat	Molecular Probes

Note: HRP: horseradish peroxidase. IB: immunoblotting. IF: immunofluorescence.

Movie S1. TIRF imaging of IFT22::HA::GFP movement in cilia of *C. reinhardtii* CC-125 cells (IFT22::HA::GFP cells). A frame from this movie and kymograph are shown in Figure 1G. Play speed is real-time (15 fps).

Movie S2. TIRF imaging of IFT22[Q69L]::HA::GFP movement in cilia of *C. reinhardtii* CC-125 cells (IFT22[Q69]::HA::GFP cells). A frame from this movie and kymograph are shown in Figure 2C. Play speed is real-time (15 fps).

Movie S3. TIRF imaging of BBS5::YFP movement in cilia of *C. reinhardtii* CC-125 cells (BBS5::YFP cells). A frame from this movie and kymograph are shown in Figure 3F. Play speed is real-time (15 fps).

Movie S4. TIRF imaging of BBS5::YFP movement in cilia of *C. reinhardtii* BBS5::YFP^{22miRNA} cells. A frame from this movie and kymograph are shown in Figure 3F. Play speed is real-time (15 fps).

Movie S5. TIRF imaging of BBS5::YFP movement in cilia of *C. reinhardtii* CC-125 cells (BBS5::YFP cells). A frame from this movie and kymograph are shown in Figure 5D. Play speed is real-time (15 fps).

Movie S6. TIRF imaging of BBS5::YFP movement in cilia of *C. reinhardtii* BBS5::YFP^{3miRNA}. A frame from this movie and kymograph are shown in Figure 5D. Play speed is real-time (15 fps).

Movie S7. TIRF imaging of BBS5::YFP movement in cilia of *C. reinhardtii* CC-5325 cells (BBS5::YFP^{5325} cells). A frame from this movie and kymograph are shown in Figure S5D. Play speed is real-time (15 fps).

Movie S8. TIRF imaging of BBS5::YFP movement in cilia of *C. reinhardtii* BBS5::YFP^{22} cells. A frame from this movie and kymograph are shown in Figure S5D. Play speed is real-time (15 fps).

SI References

1. B. Dong *et al.*, Chlamydomonas IFT25 is dispensable for flagellar assembly but required to export the BBSome from flagella. *Biol Open* **6**, 1680-1691 (2017).
2. B. Lv *et al.*, Intraflagellar transport protein IFT52 recruits IFT46 to the basal body and flagella. *J Cell Sci* **130**, 1662-1674 (2017).
3. J. Hu, X. Deng, N. Shao, G. Wang, K. Huang, Rapid construction and screening of artificial microRNA systems in Chlamydomonas reinhardtii. *Plant J* **79**, 1052-1064 (2014).
4. K. Shimogawara, S. Fujiwara, A. Grossman, H. Usuda, High-efficiency transformation of Chlamydomonas reinhardtii by electroporation. *Genetics* **148**, 1821-1828 (1998).
5. B. Zhu *et al.*, Functional exploration of the IFT-A complex in intraflagellar transport and ciliogenesis. *PLOS Genet* **13**, e1006627 (2017).
6. B. Dong *et al.*, A novel bicistronic expression system composed of the intraflagellar transport protein gene ift25 and FMDV 2A sequence directs robust nuclear gene expression in Chlamydomonas reinhardtii. *Applied Microbiol Biotech* **101**, 4227-4245 (2017).
7. Z. Wang, Z. C. Fan, S. M. Williamson, H. Qin, Intraflagellar transport (IFT) protein IFT25 is a phosphoprotein component of IFT complex B and physically interacts with IFT27 in Chlamydomonas. *PLoS One* **4**, e5384 (2009).
8. B. D. Engel *et al.*, Total internal reflection fluorescence (TIRF) microscopy of Chlamydomonas flagella. *Methods Cell Biol* **93**, 157-177 (2009).
9. B. D. Engel, W. B. Ludington, W. F. Marshall, Intraflagellar transport particle size scales inversely with flagellar length: revisiting the balance-point length control model. *J Cell Biol* **187**, 81-89 (2009).
10. Z.-C. Fan *et al.*, Chlamydomonas IFT70/CrDYF-1 Is a Core Component of IFT Particle Complex B and Is Required for Flagellar Assembly. *Mol Biol Cell* **21**, 2696-2706 (2010).
11. X. Pan, S. Eathiraj, M. Munson, D. G. Lambright, TBC-domain GAPs for Rab GTPases accelerate GTP hydrolysis by a dual-finger mechanism. *Nature* **442**, 303-306 (2006).